Journal of Zhejiang University-SCIENCE B (Biomedicine & Biotechnology) 2021 22(5):348-365
www.jzus.zju.edu.cn; www.springer.com/journal/11585
E-mail: jzus_b@zju.edu.cn

Research Article

https://doi.org/10.1631/jzus.B2000441

Protective effect of recombinant *Lactobacillus plantarum* against H_2O_2-induced oxidative stress in HUVEC cells

Guan WANG[1,2*], Mingyue HAO[1*], Qiong LIU[1], Yanlong JIANG[1], Haibin HUANG[1], Guilian YANG[1✉], Chunfeng WANG[1✉]

[1]*College of Veterinary Medicine, Jilin Provincial Engineering Research Center of Animal Probiotics, Key Laboratory of Animal Production and Product Quality Safety of Ministry of Education, Jilin Agricultural University, Changchun 130118, China*
[2]*College of Agronomy, Jilin Agricultural University, Changchun 130118, China*

Abstract: This study probed the protective effect of recombinant *Lactobacillus plantarum* against hydrogen peroxide (H_2O_2)-induced oxidative stress in human umbilical vein endothelial cells (HUVECs). We constructed a new functional *L. plantarum* (NC8-pSIP409-alr-angiotensin-converting enzyme inhibitory peptide (ACEIP)) with a double-gene-labeled non-resistant screen as an expression vector. A 3-(4, 5-dimethyl-2-thiazolyl)-2, 5-diphenyl-2H-tetrazolium bromide (MTT) colorimetric assay was carried out to determine the cell viability of HUVEC cells following pretreatment with NC8-pSIP409-alr-ACEIP. Flow cytometry (FCM) was used to determine the apoptosis rate of HUVEC cells. Cysteinyl aspartate specific proteinase (caspase)-3/8/9 activity was also assayed and western blotting was used to determine protein expression of B-cell lymphoma 2 (Bcl-2), Bcl-2-associated X protein (Bax), inducible nitric oxide synthase (iNOS), nicotinamide adenine dinucleotide phosphate oxidase 2 (gp91phox), angiotensin II (AngII), and angiotensin-converting enzyme 2 (ACE2), as well as corresponding indicators of oxidative stress, such as reactive oxygen species (ROS), mitochondrial membrane potential (MMP), malondialdehyde (MDA), and superoxide dismutase (SOD). NC8-pSIP409-alr-ACEIP attenuated H_2O_2-induced cell death, as determined by the MTT assay. NC8-pSIP409-alr-ACEIP reduced apoptosis of HUVEC cells by FCM. In addition, compared to the positive control, the oxidative stress index of the H_2O_2-induced HUVEC (Hy-HUVEC), which was pretreated by NC8-pSIP409-alr-ACEIP, iNOS, gp91phox, MDA, and ROS, was decreased obviously; SOD expression level was increased; caspase-3 or -9 was decreased, but caspase-8 did not change; Bcl-2/Bax ratio was increased; permeability changes of mitochondria were inhibited; and loss of transmembrane potential was prevented. Expression of the hypertension-related protein (AngII protein) in HUVEC cells protected by NC8-pSIP409-alr-ACEIP decreased and expression of ACE2 protein increased. These plantarum results suggested that NC8-pSIP409-alr-ACEIP protects against H_2O_2-induced injury in HUVEC cells. The mechanism for this effect is related to enhancement of antioxidant capacity and apoptosis.

Key words: Oxidative stress; Apoptosis; Human umbilical vein endothelial cell (HUVEC); Hydrogen peroxide (H_2O_2)

1 Introduction

Hypertension is the most common cardiovascular disease and one of the most important causes of death in patients with cardiovascular disease. Statistically, the total number of adult hypertension patients in the world was 1 billion in 2000, increasing to 1.13 billion in 2015 and expected to grow to 1.58 billion by 2025 (Ettinger et al., 2014; Zhou et al., 2017). In recent years, probiotics have been widely used in controlling intestinal microbiota and preventing cardiovascular disease (Upadrasta and Madempudi, 2016). As is well-known, the main drugs for treatment of hypertension have several side effects on human health (Laurent, 2017). Therefore, there is growing research interest in development of bioactive probiotics with good antihypertensive effects, high safety, and low incidence of side effects.

As an important cause of cardiovascular disease, hypertension causes stress and damage to the heart

✉ Chunfeng WANG, wangchunfeng@jlau.edu.cn
Guilian YANG, yangguilian@jlau.edu.cn
* The two authors contributed equally to this work
Guan WANG, https://orcid.org/0000-0003-0947-7086
Guilian YANG, https://orcid.org/0000-0001-5224-1592
Chunfeng WANG, https://orcid.org/0000-0002-1195-0920

Received Aug. 7, 2020; Revision accepted Dec. 23, 2020; Crosschecked Mar. 16, 2021

and other organs including the brain, liver, kidney, and blood vessel (Lugo-Baruqui et al., 2010; Wang et al., 2016). Several factors are associated with vascular endothelial cell injury, among which oxidative stress is an important cause of hypertension. Reactive oxygen species (ROS) can cause vascular endothelial cell dysfunction and damage to vascular wall cells. Antioxidant stress protects vascular endothelial cell function and prevents hypertension (Aldabbous et al., 2016; Wu et al., 2019). It has been reported that endothelial dysfunction is the source of pathogenesis of various cardiovascular diseases (Shreiber et al., 2001). When ROS is overexpressed, DNA is damaged and mitochondria have an abnormal function, which causes the inflammation and eventually induces endothelial cell apoptosis (Mendell and Olson, 2012; Wang et al., 2012). Human umbilical vein endothelial cells (HUVECs) are the most commonly used cells for in vitro research of cardiovascular and oxidative stress (Kim et al., 2018). Therefore, hypertension-induced vascular damage can be prevented by inhibiting apoptosis of HUVEC cells (Zhang Y et al., 2016). Inhibition of apoptosis is an important strategy for preventing cardiovascular diseases, including hypertension (Fraga-Silva et al., 2013; Liu et al., 2013). The exposure of HUVEC cells to hydrogen peroxide (H_2O_2) may lead to development of hypertension, and H_2O_2 may cause cardiovascular disease by promoting apoptosis of vascular endothelial cells (Wang et al., 2016; Loperena and Harrison, 2017). When HUVEC cells are exposed to H_2O_2, excessive accumulation of ROS in cells causes oxidative stress in the body, which often leads to an increase in malondialdehyde (MDA) and a decrease in superoxide dismutase (SOD) (Kim et al., 2018). Therefore, preventing apoptosis of vascular endothelial cells has positive clinical significance in the prevention and treatment of cardiovascular diseases. Several investigators have proposed the repair of vascular endothelial cell injury as part of the treatment for hypertension and believed that the degree of vascular damage may be a sign of disease severity (Small et al., 2018).

Internationally, lactic acid bacteria are regarded as the safest probiotic species. Recently, lactic acid bacteria have attracted the attention of scientists because of their potential in preventing cardiovascular disease (Upadrasta and Madempudi, 2016). It has been shown that lactic acid bacteria are effective in improving the status of cardiovascular disease, but the mechanism of their antihypertensive effect is not fully understood. Kim et al. (2018) demonstrated that lactic acid bacteria reduce hypertension by regulating intestinal microbiota and bacterial metabolites. It has been found that lactic acid bacteria regulate hypertension by controlling the content of vitamin D in the body (Yang T et al., 2015; Zittermann and Pilz, 2019). The renin-angiotensin system (RAS) is known to be an important circulating regulating system of the body. For the RAS, angiotensinogen (AGT) generates angiotensin I (AngI) under the action of renin; then AngI generates AngII under the action of angiotensin-converting enzyme (ACE); and finally AngII combines with angiotensin receptor 1 (AT1R) to form the ACE-AngII-AT1R complex that plays an important role in blood pressure regulation and water-electrolyte balance. Hypertensive patients have a chronic over-active RAS, and an increase in AngII is at the heart of events leading to fatal and disabling clinical outcomes (van Thiel et al., 2015). Lactic acid bacteria exert ACE inhibitory activity by producing antihypertensive bioactive peptides released during proteolysis, thereby mitigating hypertension by regulating RAS (Gordon, 2012; Yang T et al., 2015). As a kind of angiotensin-converting enzyme inhibitor, ACEI is widely used due to its minimal side effects, but patients using the synthetic ACEI drugs currently on the market often experience the side effect of a persistent dry cough caused by increased concentration of bradykinin (Graham et al., 2004). Compared with synthetic antihypertensive drugs, the natural ACE inhibitory peptide prepared by genetic engineering has high safety, with no toxic side effects or excessive antihypertensive effects; thus, there is growing research interest in the therapeutic possibilities of the natural peptide. In recent years, probiotic-containing foods have become increasingly popular in related industries because of increased consumer awareness of the probiotic benefits of health foods (Pavli et al., 2018).

H_2O_2 produces a large number of ROS, thereby causing oxidative damage to vascular endothelial cells, inducing apoptosis, and promoting development of hypertension (Korsager Larsen and Matchkov, 2016). Our laboratory has successfully constructed a recombinant *Lactobacillus plantarum* expressing antihypertensive peptide (NC8-pSIP409-angiotensin-converting enzyme inhibitory peptide (ACEIP)) and shown that administration of this *L. plantarum* lowers blood pressure (Yang GL et al., 2015). Considering the possibility that erythromycin resistance may affect patients in

subsequent applications, in this study we have optimized NC8-pSIP409-ACEIP and adapted the non-resistant expression vector maintained in our laboratory to construct a new functional recombinant *L. plantarum* (NC8-pSIP409-alr-ACEIP) with ACEIP fusion protein screened for non-resistance. We investigated the protective effect of NC8-pSIP409-alr-ACEIP against oxidative damage due to H_2O_2 using HUVEC cells.

2 Materials and methods

2.1 Cell lines and culture

HUVEC cell lines were obtained from the Chinese Academy of Sciences Cell Bank (Shanghai, China). HUVEC cells were cultured in Roswell Park Memorial Institute-1640 (RPMI-1640) supplemented with 10% fetal bovine serum (FBS), 100 μg/mL penicillin, and 100 μg/mL streptomycin, and then placed into an incubator with 5% CO_2 at 37 °C. The cells were grown up to 80% confluency and passaged every 2−3 d. The cells were sub-cultured, and cells in the logarithmic phase were used in the assays.

2.2 Bacterial strains and plasmids

The bacterial strains and plasmids used in this study have been described previously (Yang GL et al., 2015). NC8-alr was a non-resistant vector lacking D-alanine racemase gene. *asd-alr* fusion genes were used as nutritional complementary type screening markers, PLp_1261Inv of a screening marker with *erm* resistance genes was the basic vector, and the *erm* resistance genes on the vector were replaced by *asd-alr* fusion genes. The anchoring expression plasmid NC8-alr with non-resistant screening marker was constructed. NC8-alr was cultured in de Man Rogosa and Sharpe (MRS) medium containing 100 mg/mL of D-alanine at 37 °C under anaerobic conditions, which was preserved by the Jilin Provincial Animal Microecological Preparation Engineering Research Center (Changchun, China).

2.3 Chemicals and materials

H_2O_2 and dimethyl sulfoxide (DMSO) were obtained from MP Biomedica (California, USA). RPMI-1640, FBS, phosphate-buffered saline (PBS), 0.25% (2.5 g/L) trypsase, penicillin-streptomycin, and 3-(4,5-dimethyl-2-thiazolyl)-2,5-diphenyl-2H-tetrazolium bromide (MTT) were purchased from Hyclone Laboratories (Logan, USA). The fluorescein isothiocyanate (FITC) Annexin V Apoptosis Detection Kit I was purchased from BD Pharmingen (New Jersey, USA). Other experimental chemical reagents were purchased from Beyotime Institute of Biotechnology (Shanghai, China). All antibodies were purchased from Proteintech (Wuhan, China).

2.4 Construction of non-resistant recombinant *L. plantarum* NC8-pSIP409-alr-ACEIP expressing ACEIP fusion protein

First, the erythromycin resistance gene was deleted from the original recombinant strain; next, the gene expressing the ACEIP fusion protein was introduced into the recombinant strain to create a non-resistant recombinant *L. plantarum* NC8-pSIP409-alr-ACEIP. Since the plasmid carries the gene for D-alanine racemase expression, D-alanine was not added to the MRS solid medium in screening for positive bacteria. Positive bacteria were picked and incubated in MRS liquid medium overnight; plasmids were prepared in small quantities and identified by *Bam*HI/*Nco*I digestion, and sequenced by Comate Bioscience Co., Ltd. (Changchun, China). Western blot was used to verify protein expression of NC8-pSIP409-alr-ACEIP by following specific procedural steps. First, sake lactobacillin sakasin-P (sPPIP) was added to induce overnight growth of a 50-mL bacterial solution. After sonication, the bacterial solution was centrifuged (1000*g* for 10 min at 4 °C). Next, the resulting supernatant was mixed with 5× loading buffer at 5:1 (volume ratio (v/v)) and the precipitate was mixed with PBS and then mixed with 5× loading buffer at 5:1 (v/v). The protein samples were separated by sodium dodecyl sulfate-polyacrylamide gel electrophoresis (SDS-PAGE) with a 17% (0.17 g/mL) gel, transferred to a membrane for 1 h, blocked with skim milk for 3 h, and incubated with the primary antibody (6×His, His-Tag monoclonal antibody (Proteintech, 66005-1-Ig)) overnight. The next day, the membrane was washed three times in SDS buffer on a shaker for 10 min apiece. The membrane was then incubated with the secondary antibody (horse radish peroxidase (HRP)-conjugated AffiniPure goat anti-mouse IgG (H+L) (Proteintech, SA00001-1)) for 1 h at 4 °C and washed with SDS buffer three times, with each time for 10 min on a shaker. Finally, samples were analyzed by the western blot imaging system AI600 (Thermo Fisher Scientific, Shanghai, China).

2.5 Establishment of an oxidative stress injury cell model using H_2O_2

A cell model of oxidative stress was established using H_2O_2 (named H_2O_2-induced HUVEC (Hy-HUVEC)). We used the MTT assay to determine the effect of different concentrations of H_2O_2 on cytosine in HUVEC cells. HUVEC cells were seeded at 7000 cells/well into 96-well plates and incubated overnight. H_2O_2 was added to a final concentration of 100, 200, 300, 400, 500, 600, 700, or 800 μmol/L in a volume of 200 μL per well. After further incubation for 1 or 2 h, 20 μL of MTT reagent was added to each well and cells were incubated for 4 h. Next, the medium was replaced by 150 μL of DMSO. A BioTek Epoch 2 Microplate Spectrophotometer (BioTek, Vermont, USA) was used to assess absorbance at 492 nm using a 96-well plate reader. We confirmed the best concentration of H_2O_2 for the cell model using the MTT assay. The viability of HUVEC cells was calculated with the following equation: cell viability=(OD of experimental group)/(OD of control)×100% (Präbst et al., 2017), where OD is the optical density.

2.6 Cytotoxic effect of NC8-pSIP409-alr-ACEIP in HUVEC cells

The MTT assay was used to assess the cytotoxic effects of NC8-pSIP409-alr-ACEIP on HUVEC cells. After HUVEC cells were digested, samples were diluted with complete RPMI-1640 culture medium. The cells were seeded at 7000 cells/well onto 96-well plates and incubated overnight. Next, the medium was replaced at NC8-pSIP409-alr-ACEIP/HUVEC ratio of 20:1, 40:1, 80:1, 160:1, or 320:1 in a volume of 200 μL per well; cells were then centrifuged at 3000*g* for 10 min to bring NC8-pSIP409-alr-ACEIP into close contact with HUVEC cells. The control group consisted of a series of cells with the same ratios of medium to NC8-alr (*L. plantarum* empty vector). After centrifugation, the cells were further incubated for 1 or 3 h at 37 °C. Each well was incubated with 20 μL MTT reagent for 4 h. DMSO (150 μL) was added to each well after discard of medium.

2.7 Cell viability assay

HUVEC cells were pretreated with NC8-pSIP409-alr-ACEIP (20:1, 40:1, 80:1, 160:1, and 320:1) followed by exposure to H_2O_2 (800 μmol/L). Cell viability was measured by MTT assay.

2.8 Determination of apoptotic rate of HUVEC cells induced by NC8-pSIP409-alr-ACEIP

Cell apoptosis rate was determined using the Annexin V-FITC/propidium iodide (PI) double labeling method with flow cytometry (FCM). In brief, HUVEC cells (2×10^5 cells/mL) were seeded at 2 mL/well onto six-well plates. After overnight incubation, NC8-pSIP409-alr-ACEIP was added at a bacterium/cell ratio of 20:1, 40:1, 80:1, 160:1, or 320:1 in a volume of 2 mL per well and incubated for 2 h. NC8-alr was added to the control group at the same ratios as the treatment group. A concentration of 800 μmol/L H_2O_2 was used as a positive control. Next, the cells were harvested and washed with ice-cold PBS, and adjusted to 1×10^6 cells/mL with 1× binding buffer. The cell suspension (100 μL) was loaded into a solution containing 15 μL Annexin V-FITC and 5 μL PI (Bestbio, Shanghai, China), gently mixed, and incubated in the dark at 4 °C for 20 min. After staining, the cells were washed with PBS containing 0.5% (5 g/L) FBS. Finally, the cells were resuspended in 400 μL binding buffer. After filtration, suspensions of each treatment group were analyzed with a BD FACSCalibur (Becton, Dickinson and Company, New Jersey, USA).

2.9 Measurement of intracellular ROS

Intracellular ROS concentration was monitored spectrofluorimetrically using an oxidation-sensitive 2',7'-dichlorofluorescein diacetate (no fluorescence) (DCFH-DA) probe (Wan et al., 2011). Hy-HUVEC cells (2×10^5 cells/mL) were seeded at 2 mL/well onto six-well plates. NC8-pSIP409-alr-ACEIP and NC8-alr were added to the experimental and control Hy-HUVEC cells, respectively, at a bacterium/cell ratio of 20:1, 40:1, 80:1, 160:1, or 320:1 in a volume of 2 mL per well and incubated for 2 h. The bacterial suspension was decanted and then washed with ice-cold PBS. Cells were collected and incubated with 2 μmol/L (final concentration) DCFH-DA or 2',7'-dichlorofluorescein diacetate (with fluorescence) (DCF-DA) for 20 min at 37 °C. Loaded cells were washed three times and the fluorescence intensity of DCF was determined using a fluorescence microscope (LEICA DMi8, Germany) with an excitation wavelength of 485 nm and emission wavelength of 538 nm. The relative amount of intracellular ROS production was expressed as the fluorescence ratio of treatment to control values.

2.10 Determining the mitochondrial membrane potential (MMP) change

HUVEC cells were harvested at a robust logarithmic growth phase, inoculated into six-well plates after digestion, and cultured for 24 h. Next, 800 μmol/L of H_2O_2 was added and cells were incubated for 1 h; they were then incubated in 160:1 (v/v) NC8-pSIP409-alr-ACEIP (experimental groups) and NC8-alr (controls) for 2 h. Next, medium was removed from each well, and cells were washed with fresh RPMI-1640; a working solution of JC-10 stain was then added, mixed well, and incubated at 37 °C for 20 min. During incubation, 1 mL of JC-10 (5×) buffer was diluted with 4 mL water and added to each well, and then placed in an ice bath. After incubation for 20 min, the supernatant of each well was aspirated; cells were washed twice with buffer followed by addition of 2 mL of fresh RPMI-1640, and then observed under a fluorescence microscope.

2.11 Intracellular SOD and MDA activity assay

The Hy-HUVEC cells were treated as described above. Cells were washed once with pre-cooled PBS; 200 μL of sample preparation solution was added to 1×10^6 cells and appropriately lysed the cells. A WST-8/enzyme working solution was prepared using 151 μL SOD detection buffer+8 μL WST-8+1 μL enzyme solution for each reaction volume of 160 μL. The starting solution contained 1 μL of reaction starter (40×) and 39 μL SOD assay buffer. After solution preparation, 20 μL of the sample to be tested was added to each well of the 96-well plate, and 160 μL of working solution was added to each well, followed by addition of 20 μL of the starting solution; reactions were carried out on ice. Control group 1 used 20 μL SOD buffer, 160 μL working fluid, and 20 μL starting solution. Control group 2 used 40 μL SOD buffer and 160 μL working solution. After incubation at 37 °C for 30 min, absorbance at 450 nm was read using a microplate reader. All cells were treated in the same way: washed once with pre-chilled PBS, digested with trypsin, and mixed with pre-chilled PBS (100 μL of PBS added per 1×10^6 cells) and shaken for 1 min with a vortex shaker. The supernatant was collected after centrifugation for 10 min at 12 000*g* (all of the above steps were performed on ice). Thiobarbituric acid (TBA) stock solution standards were prepared according to MDA instructions. After mixing of control, experimental, and reference solutions, samples were boiled at 100 °C for 15 min, cooled to room temperature in water bath, and centrifuged at 1000*g* for 10 min. Supernatant (200 μL) was added to each well of a 96-well plate and absorbance at 532 nm was measured with a BioTek Epoch 2 microplate spectrophotometer.

2.12 Measuring caspase-3, -8, and -9 activity in Hy-HUVEC cells

The Hy-HUVEC cells were treated as described above. Activities of caspase-3, -8, and -9 were determined using the caspase-3, -8, and -9 activity kits (Beyotime, Shanghai, China). Cells were collected by centrifugation at 600*g* for 5 min at 4 °C, and the supernatant was carefully aspirated, while ensuring that as few cells as possible were removed; the cell pellet was washed once with PBS. After the supernatant was aspirated, 80 μL of the lysing reagent was added, the pellet was resuspended and lysed for 15 min in an ice bath. The suspension was centrifuged at 18 000*g* for 15 min at 4 °C. Then, the supernatant from each sample was collected and loaded into an ice-cold centrifuge tube. The reaction system was set up according to the instructions of the caspase-3 activity assay kit, and the detection buffer, the sample to be tested, the lysate, and acetyl-Asp-Glu-Val-Asp-*p*-nitroanilide (Ac-DEVD-pNA; 2 mmol/L) were assigned to a blank group and a detection group. Ac-DEVD-pNA (2 mmol/L) was added to each sample and mixed well, taking care to avoid air bubbles when mixing; samples were incubated for 120 min at 37 °C. Caspase-3 activity was measured immediately at 405 nm using a BioTek Epoch 2 microplate spectrophotometer. For caspase-8 assays, Ac-DEVD-pNA (2 mmol/L) was replaced with acetyl-Ile-Glu-Thr-Asp-p-nitroanilide (Ac-IETD-pNA; 2 mmol/L), and the rest of the conditions were unchanged. For caspase-9 experiments, Ac-DEVD-pNA (2 mmol/L) was replaced with Ac-LEHD-pNA (2 mmol/L), and the rest of the conditions were unchanged.

2.13 Western blotting of related proteins

The Hy-HUVEC cells were treated as described above (see Section 2.8), washed twice with ice-cold PBS, and gently lysed for 1 h in ice-cold cell lysis buffer. Lysates were centrifuged at 12 000*g* at 4 °C for 10 min. Supernatants were collected to determine protein concentrations for western blotting analysis. An equal amount of protein was subjected to SDS-PAGE

and transferred to a polyvinylidene fluoride (PVDF) membrane by electroblotting. The blots were blocked in PBS containing 10% non-fat milk and 0.1% Tween-20 (blotting grade) for 3 h and then applied to probe the desired antibodies at 4 ℃ overnight. Membranes were subsequently incubated with appropriate HRP-conjugated secondary antibody for 45 min and visualized by western blotting detection reagents. Loading differences were normalized using a monoclonal β-actin antibody.

2.14 Statistical analysis

All experiments were performed in triplicate unless otherwise indicated. Results are expressed as the means of three independent experiments. All data were expressed as the mean±standard error of the mean (SEM). Statistical analysis was performed using a two-tailed Student's *t*-test with GraphPad Prism 5.0 (GraphPad Software, California, USA).

3 Results

3.1 Construction of non-resistant recombinant *L. plantarum* NC8-pSIP409-alr-ACEIP expressing ACEIP fusion protein

Non-resistant recombinant *L. plantarum* NC8-pSIP409-alr-ACEIP expressing the ACEIP fusion protein was successfully constructed in this study (Fig. 1a). NC8-pSIP409-alr-ACEIP was digested by *Nco*I and *Bam*HI to obtain two fragments: a 5808-bp fragment of vector and a 1988-bp fragment of target gene (Fig. 1b). Next, the target gene was cloned into an expression vector and sequenced by Comate Bioscience Co., Ltd. (Changchun, China). The sequencing results showed 100% homology using BLAST. In addition, western blotting results indicated that a specific protein band of approximately 8.5 kDa was expressed in *L. plantarum*. After successful expression of the ACEIP protein (Fig. 1c), the growth curve was analyzed to determine when the inducible peptide sPPIP should be added and to select the best point for optimal bacterial growth expression. Fig. 1d indicates that the bacteria increased exponentially at 4−6 h after addition of the inducible peptide sPPIP. Therefore, in this study, the bacteria were collected at 4.5 h and then measured by the drop plate counting method for subsequent experiments.

3.2 Construction of an oxidative stress-injury cell model using Hy-HUVEC

The MTT method was used to select an appropriate concentration of H_2O_2 for the HUVEC cell model. A previous study (Wu et al., 2018) suggested H_2O_2 concentrations ranging from 100 to 800 μmol/L with 1 or 3 h treatment period. Our data indicated that proliferation of HUVEC cells was effectively inhibited by H_2O_2 in both a dose- and time-dependent manner (Fig. 2). With 400 μmol/L H_2O_2 treatment, HUVEC cells had a survival rate of 84% and 76% after 1 and 3 h incubation, respectively. Furthermore, only 48% of the cells survived when H_2O_2 concentration increased to 800 μmol/L under 1-h treatment, a result approximating the half maximal inhibitory concentration. Similarly, the cell survival rate was 45% with 3 h incubation at 600 μmol/L. Considering the time cost, we chose a treatment of 800 μmol/L H_2O_2 for 1 h to establish the an oxidative stress-injury cell model (Hy-HUVEC).

3.3 Analysis of toxicity test results of NC8-pSIP409-alr-ACEIP on HUVEC cells

To test whether NC8-alr and NC8-pSIP409-alr-ACEIP are toxic to HUVEC cells, the survival rates of HUVEC cells incubated with NC8-pSIP409-alr-ACEIP and NC8-alr were determined by MTT assay. As seen in Fig. 3, neither NC8-pSIP409-alr-ACEIP nor NC8-alr had any effect on the survival rate of HUVEC cells. Instead, an increase in the proportion of recombinant *L. plantarum* and the prolongation of incubation time promoted cell growth, with 2-h incubation yielding greater cell growth than 1-h incubation. These results suggested that both bacterial strains were basically non-toxic and could be used in subsequent experiments.

3.4 Effect of NC8-pSIP409-alr-ACEIP on H_2O_2-indued injury in HUVEC cells

NC8-pSIP409-alr-ACEIP was added to Hy-HUVEC cells and incubated for either 1 or 2 h. As shown in Fig. 4, the average survival rate of Hy-HUVEC cells was (57.78±0.40)% after 1-h protection, with adding NC8-pSIP409-alr-ACEIP at a ratio of 20:1, which was slightly higher than that of the positive control group. Cell survival was significantly increased to (70.55±0.70)% after 1-h incubation, when the ratio was increased to 320:1. When incubation time was

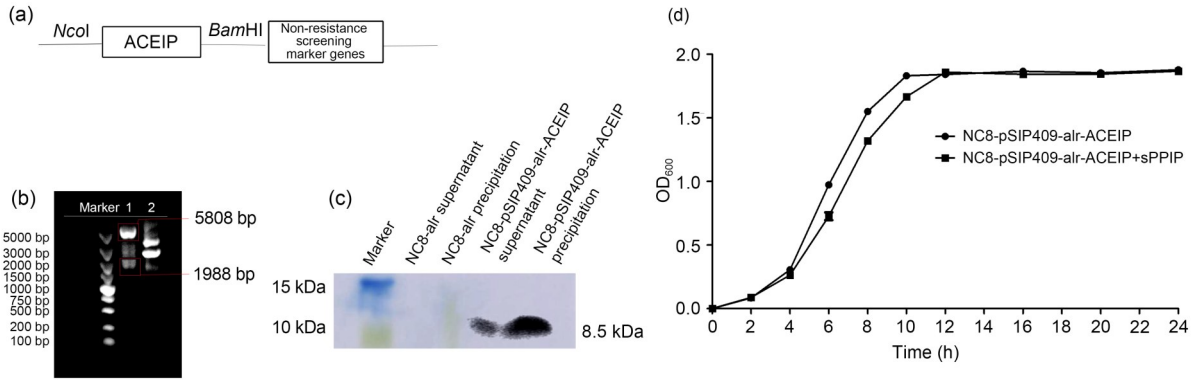

Fig. 1 Schematic diagram of NC8-pSIP409-alr-ACEIP construction and expression. (a) Schematic diagram of ACEIP recombinant expression vector. (b) Agarose gel electrophoresis of plasmid. Plasmid digested by restriction enzymes pla*Nco*I and *Bam*HI (Lane 1) and undigested plasmid (Lane 2) were run on agarose gel and expected bands are shown (5808 bp for vector and 1988 bp for target gene). (c) Western blot determined that ACEIP fusion protein was successfully expressed in NC8-pSIP409-alr. (d) Growth curve of recombinant *Lactobacillus plantarum* NC8-pSIP409-alr-ACEIP. ACEIP: angiotensin-converting enzyme inhibitory peptide; OD_{600}: optical density at 600 nm.

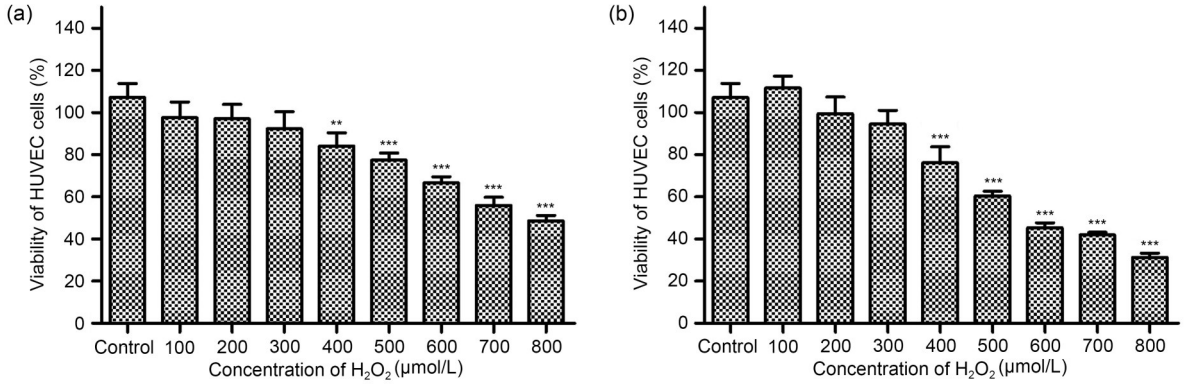

Fig. 2 Effects of H_2O_2 on HUVEC cell growth. Cells were seeded at a density of 7000 cells/well and then treated with 100, 200, 300, 400, 500, 600, 700, and 800 μmol/L H_2O_2 for 1 h (a) or 3 h (b). The control group was treated with RPMI-1640. Cell viability was then determined by MTT assay. Data are presented as mean±standard deviation (SD) with three independent experiments. $^{**}P<0.01$, $^{***}P<0.001$, compared with the control.

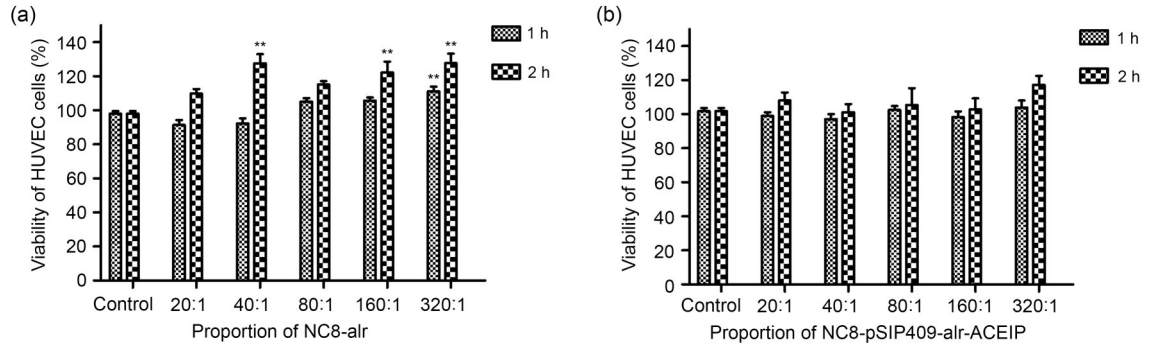

Fig. 3 Effects of NC8-alr (a) or NC8-pSIP409-alr-ACEIP (b) on HUVEC cell growth. Cells were seeded at a density of 7000 cells/well and then treated at bacterium/cell ratios of 20:1, 40:1, 80:1, 160:1, and 320:1 for 1 or 2 h. The control group was treated with RPMI-1640. Cell viability was then determined by MTT assay. Data are presented as mean±standard deviation (SD) with three independent experiments. $^{**}P<0.01$, compared with the control. ACEIP: angiotensin-converting enzyme inhibitory peptide.

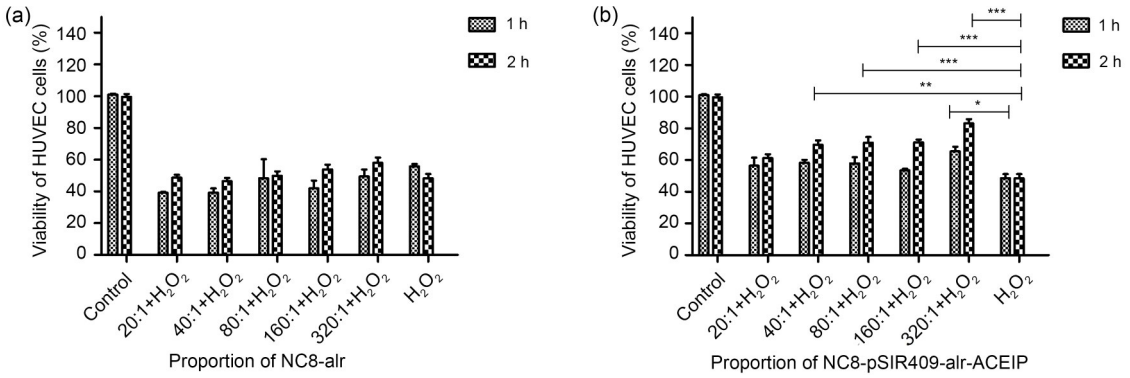

Fig. 4 Cell viabilities of Hy-HUVEC treated with NC8-alr (a) or NC8-pSIP409-alr-ACEIP (b) for 1 or 2 h determined by MTT assay. NC8-pSIP409-alr-ACEIP promotes proliferation of Hy-HUVEC cells. Cells were plated in the 96-well plates at 7000 cells/well. Next, the cells were treated with bacterium/Hy-HUVEC ratios of 20:1, 40:1, 80:1, 160:1, and 320:1 for 1 and 2 h, while the control group was treated with RPMI-1640. Data are presented as mean±standard deviation (SD) with three independent experiments. * $P<0.05$, ** $P<0.01$, *** $P<0.001$, compared with the positive H_2O_2 control group. ACEIP: angiotensin-converting enzyme inhibitory peptide; Hy-HUVEC: H_2O_2-induced human umbilical vein endothelial cell.

extended to 2 h, cell viability was significantly improved. Cell survival rate was (67.58±0.30)% when NC8-pSIP409-alr-ACEIP was added at a ratio of 160:1 under 2-h incubation. Conducting the same experiment with the empty vector NC8-alr demonstrated that NC8-alr has no protective effect on Hy-HUVEC cells. Therefore, we hypothesized that the protective effect of NC8-pSIP409-alr-ACEIP on Hy-HUVEC cells is due to the expression of ACEIP fusion protein.

3.5 Effect of NC8-pSIP409-alr-ACEIP on apoptosis by H_2O_2-indued injury in HUVEC cells

Apoptosis is a process of programmed cell death that involves a series of biochemical events. As a follow-up to the cytotoxic effect experiment, FCM was used to understand in more detail the mechanism that NC8-pSIP409-alr-ACEIP was used to inhibit Hy-HUVEC cell growth. Live cells were not stained after treatment with Annexin V-FITC and PI. Early apoptotic cells were stained with Annexin V-FITC, but not with PI. Necrotic and late apoptotic cells were stained with both Annexin V-FITC and PI. Therefore, to detect apoptosis, the cells were treated with different bacterium/cell ratios for 2 h, and then prepared for apoptosis analysis via FCM (Fig. 5). Consistent with previous MTT assay results, FCM analysis showed that NC8-pSIP409-alr-ACEIP or NC8-alr had little effect on the cells regardless of concentration. The results further confirmed the above findings (Fig. 3), indicating that recombinant *L. plantarum* had no toxic effects on cells. Next, the apoptotic rate of Hy-HUVEC cells was determined. The results showed that the apoptotic rate of the positive control group with H_2O_2 treatment was greater than 70.4% and significantly decreased after adding NC8-pSIP409-alr-ACEIP for 2 h. When the bacterium/cell ratio reached 160:1, the apoptotic rate of Hy-HUVEC cells had a dose-dependent decrease to 31.2%. Similarly, the apoptotic rate of Hy-HUVEC cells also decreased after 2 h of NC8-alr incubation. When the bacterium/cell ratio reached 160:1, the apoptotic rate of Hy-HUVEC cells was 57.1% with a non-dose-dependent manner, and rates of both early and late apoptosis were lower in the 160:1 group than in the 320:1 group. Based on the above results, we chose a ratio of 160:1 and 2 h treatment as the experimental conditions for our experimental tests. Although NC8-alr had a somewhat protective effect, the effect was still much lower than that of NC8-pSIP409-alr-ACEIP. Therefore, according to the above results, we further confirmed that NC8-pSIP409-alr-ACEIP has a protective effect and that it reduces apoptosis in Hy-HUVEC cells.

3.6 Effect of NC8-pSIP409-alr-ACEIP on ROS level

ROS levels in Hy-HUVEC cells were determined with a DCFH-DA fluorescent probe (Fig. 6). Under the fluorescence microscope, the DCF signal was significantly increased and green fluorescence was significantly increased in the H_2O_2 positive control group (Fig. 6b) compared with the control group (Fig. 6a). However, fluorescence intensity was significantly decreased after treatment with NC8-alr+H_2O_2 (Fig. 6e) and NC8-pSIP409-alr-ACEIP+H_2O_2 (Fig. 6f). These data

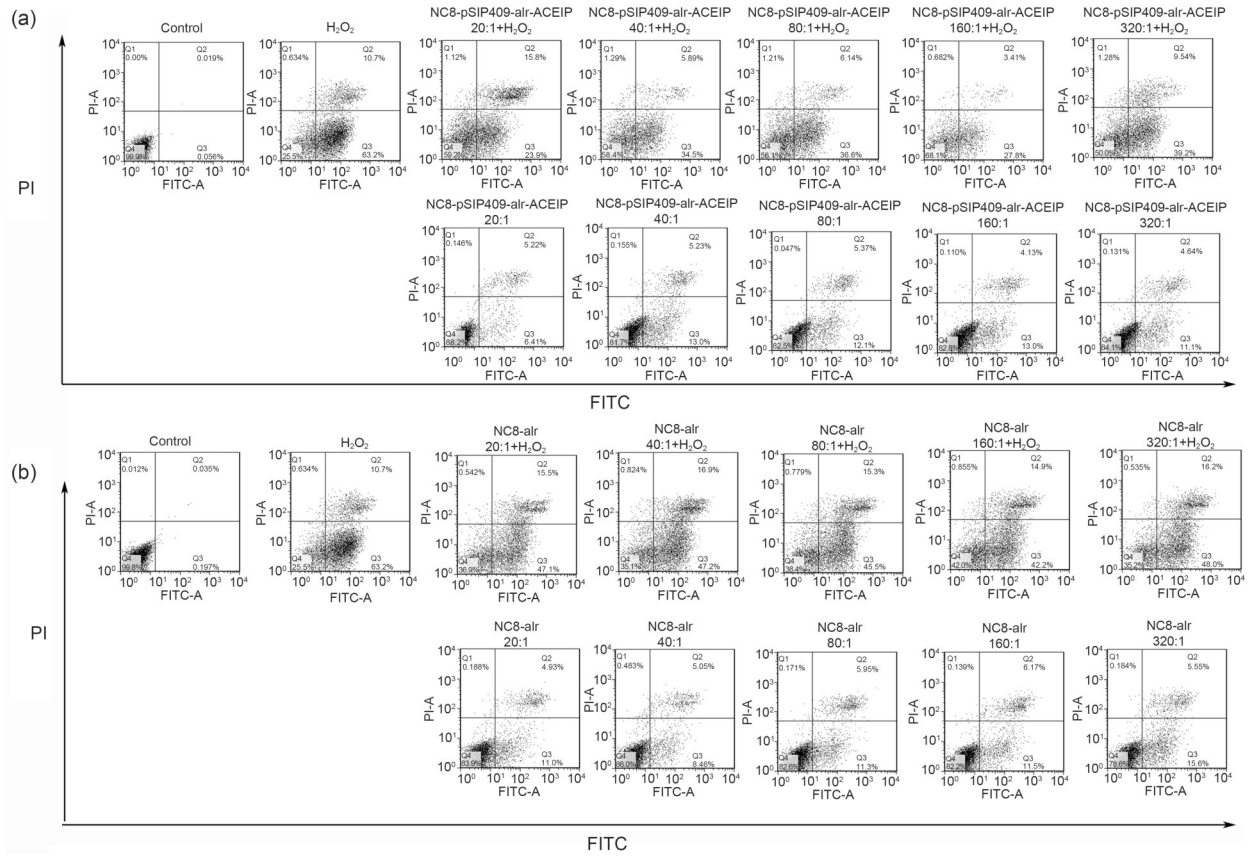

Fig. 5 Flow cytometric analysis of apoptotic Hy-HUVEC cells induced by NC8-pSIP409-alr-ACEIP. Hy-HUVEC cells were treated with NC8-pSIP409-alr-ACEIP (a) or NC8-alr (b), which was added at bacterium/cell ratios of 20:1, 40:1, 80:1, 160:1, and 320:1 for 2 h. FITC: fluorescein isothiocyanate; PI: propidium iodide; ACEIP: angiotensin-converting enzyme inhibitory peptide.

suggested that both NC8-alr and NC8-pSIP409-alr-ACEIP could reduce ROS levels. However, compared with NC8-pSIP409-alr-ACEIP, NC8-alr clearly shows a less decrease in fluorescence, that is, a lower inhibiting effect on apoptosis. There is also no apparent difference in fluorescence between the control group (without H_2O_2) and the group with addition of only NC8-alr (Fig. 6c) or NC8-pSIP409-alr-ACEIP (Fig. 6d). These results indicated that the ROS levels in Hy-HUVEC cells were significantly reduced after treatment with NC8-pSIP409-alr-ACEIP.

3.7 Effect of NC8-pSIP409-alr-ACEIP treatment on the MMP

To further investigate the effects of NC8-pSIP409-alr-ACEIP on Hy-HUVEC cells, we assayed MMP in these cells. As shown in Fig. 7, red fluorescence intensity was significantly decreased in the H_2O_2 positive control group (Fig. 7b) compared to the control group (Fig. 7a). When NC8-pSIP409-alr-ACEIP+H_2O_2 was added to the HUVEC cells (Fig. 7f), red fluorescence intensity in the cells was significantly enhanced, similar to that of the control group (Fig. 7a). However, the intracellular red fluorescence intensity of the NC8-alr+H_2O_2 group (Fig. 7e) was weaker than that of the NC8-pSIP409-alr-ACEIP+H_2O_2 group (Fig. 7f). Green fluorescence intensity was significantly reduced in both the NC8-pSIP409-alr-ACEIP+H_2O_2 (Fig. 7f) and NC8-alr+H_2O_2 (Fig. 7e) groups, and in both groups was similar to that of the control group (Fig. 7a). Green fluorescence intensity was enhanced in the H_2O_2 positive control group (Fig. 7b) compared with the control group (Fig. 7a). After the addition of NC8-alr+H_2O_2 (Fig. 7e) and NC8-pSIP409-alr-ACEIP+H_2O_2 (Fig. 7f) protection, green fluorescence intensity was significantly weakened, approaching that of the control group (Fig. 7a). Surprisingly, the green fluorescence intensity of the NC8-alr+H_2O_2 group (Fig. 7e) was stronger than that of the

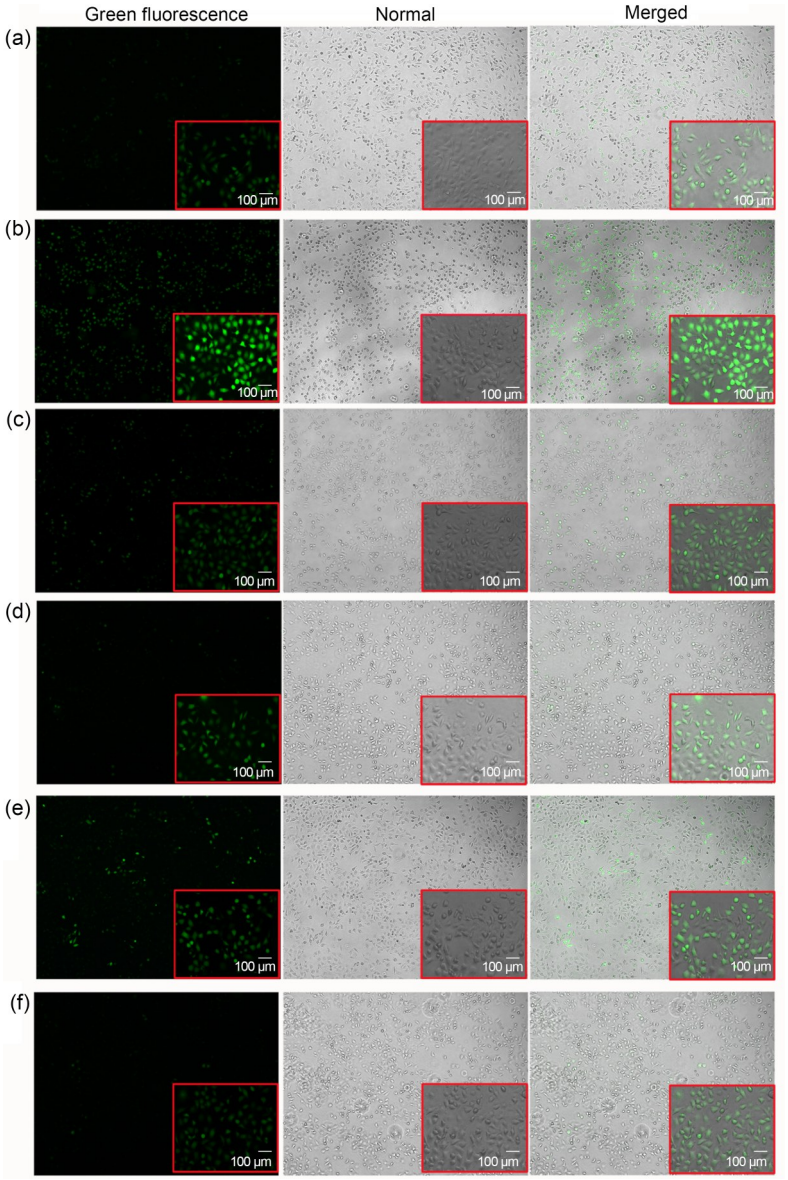

Fig. 6 Analysis of ROS levels in Hy-HUVEC cells with NC8-pSIP409-alr-ACEIP treatment. ROS generation in the control and Hy-HUVEC cells was assayed with DCFH-DA. Fluorescence intensity of the oxidation-insensitive probed DCF-DA in control and Hy-HUVEC cells was measured. Cells were examined under a fluorescence microscope. The large images and small images were observed under field of view of 5× and 20× magnifications (scale bar=100 μm), respectively. (a) Control group; (b) H_2O_2 positive control group; (c) NC8-alr group; (d) NC8-pSIP409-alr-ACEIP group; (e) NC8-alr+H_2O_2 group; (f) NC8-pSIP409-alr-ACEIP+H_2O_2 group. When ROS levels were increased in cells, the DCF signal was increased and the intensity of green fluorescence was enhanced. The intensity of the green fluorescence can be regarded as an indicator of ROS level. Hy-HUVEC: H_2O_2-induced human umbilical vein endothelial cell; ACEIP: angiotensin-converting enzyme inhibitory peptide; ROS: reactive oxygen species; DCFH-DA: 2',7'-dichlorofluorescein diacetate (no fluorescence); DCF-DA: 2',7'-dichlorofluorescein diacetate (with fluorescence) (Note: for interpretation of the references to color in this figure legend, the reader is referred to the web version of this article).

NC8-pSIP409-alr-ACEIP+H_2O_2 group (Fig. 7f). Compared with the control group, there was no difference in either the NC8-alr group (Fig. 7c) or NC8-pSIP409-alr-ACEIP group (Fig. 7d). Finally, in the merged green and red fluorescence images, the fluorescence was red in the control group (Fig. 7a) and was green in the H_2O_2 positive control group (Fig. 7b). After addition of NC8-alr+H_2O_2 (Fig. 7e) and NC8-pSIP409-alr-ACEIP+H_2O_2 (Fig. 7f), the fluorescence in the cells was orange-red, approaching that of the control group (Fig. 7a), and

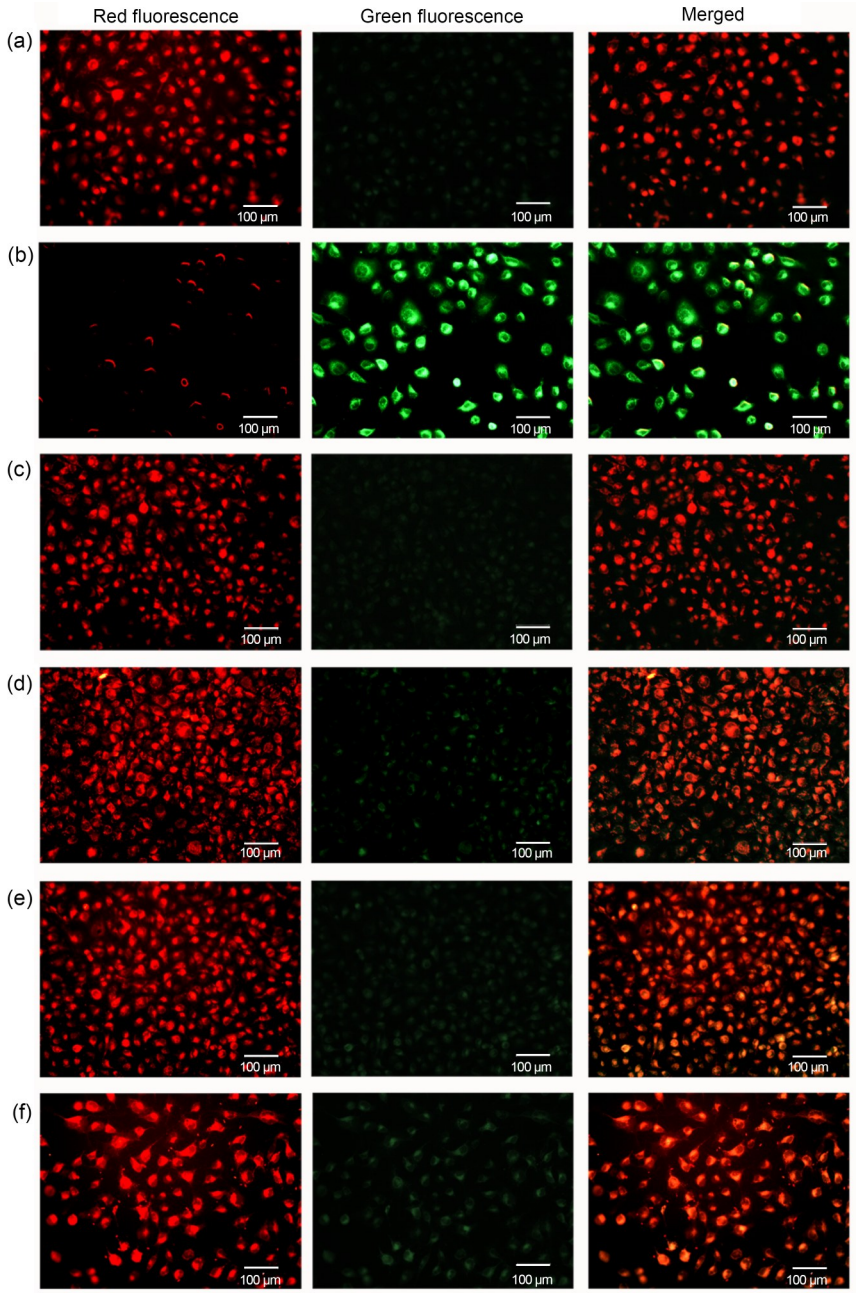

Fig. 7 Effects of NC8-pSIP409-alr-ACEIP on MMP in Hy-HUVEC cells. Cells treated with NC8-pSIP409-alr-ACEIP (bacterium/cell ratio: 160:1) were incubated with JC-10, and their fluorescence intensity was measured. (a) Control group; (b) H_2O_2 positive control group; (c) NC8-alr group; (d) NC8-pSIP409-alr-ACEIP group; (e) NC8-alr+H_2O_2 group; (f) NC8-pSIP409-alr-ACEIP+H_2O_2 group. There was a significant difference in fluorescence between the H_2O_2-treated cells (b) and the NC8-pSIP409-alr-ACEIP-treated cells (f). Hy-HUVEC: H_2O_2-induced human umbilical vein endothelial cell; ACEIP: angiotensin-converting enzyme inhibitory peptide; MMP: mitochondrial membrane potential. Scale bar=100 μm (Note: for interpretation of the references to color in this figure legend, the reader is referred to the web version of this article).

the fluorescence intensity was weaker in the NC8-alr+H_2O_2 group (Fig. 7e) than in the NC8-pSIP409-alr-ACEIP+H_2O_2 group (Fig. 7f). Compared with the control group, there was no difference in the NC8-alr group (Fig. 7c) or the NC8-pSIP409-alr-ACEI group (Fig. 7d). Above all, the results indicated that after pretreatment with NC8-alr and NC8-pSIP409-alr-ACEIP, MMP began to repolarize and gradually returned to its normal

state, and NC8-pSIP409-alr-ACEIP was superior in its effect to that of NC8-alr.

3.8 Effects of NC8-pSIP409-alr-ACEIP on anti-oxidation-related indicators

Oxidative stress often leads to a decrease in SOD activity and an increase in MDA content. Expression levels of inducible nitric oxide synthase (iNOS) and nicotinamide adenine dinucleotide phosphate oxidase 2 (gp91phox) are also increased. To investigate the effect of NC8-pSIP409-alr-ACEIP on the antioxidant capability of Hy-HUVEC cells, we assayed SOD activity and content of MDA. The activity of SOD and the content of MDA are shown in Figs. 8a and 8b. There was a decrease in the SOD activity in the H_2O_2 positive control group. After the pretreatment with NC8-pSIP409-alr-ACEIP and NC8-alr, the SOD activity in Hy-HUVEC cells had an increase, and the NC8-pSIP409-alr-ACEIP group exhibited better protection effect than the NC8-alr group (Fig. 8a). At the same time, MDA content in the H_2O_2 positive control group was significantly higher than that in the negative control group (Fig. 8b), and the MDA content in the cells was decreased after NC8-alr and NC8-pSIP409-alr-ACEIP treatments. MDA content of the NC8-pSIP409-alr-ACEIP+H_2O_2 group was significantly decreased, which corresponds to the SOD results. These two results demonstrate that NC8-pSIP409-alr-ACEIP has a good antioxidant effect and is superior to NC8-alr. The non-phagocytic cell oxidase (NOX) proteins of NADPH oxidase are widely

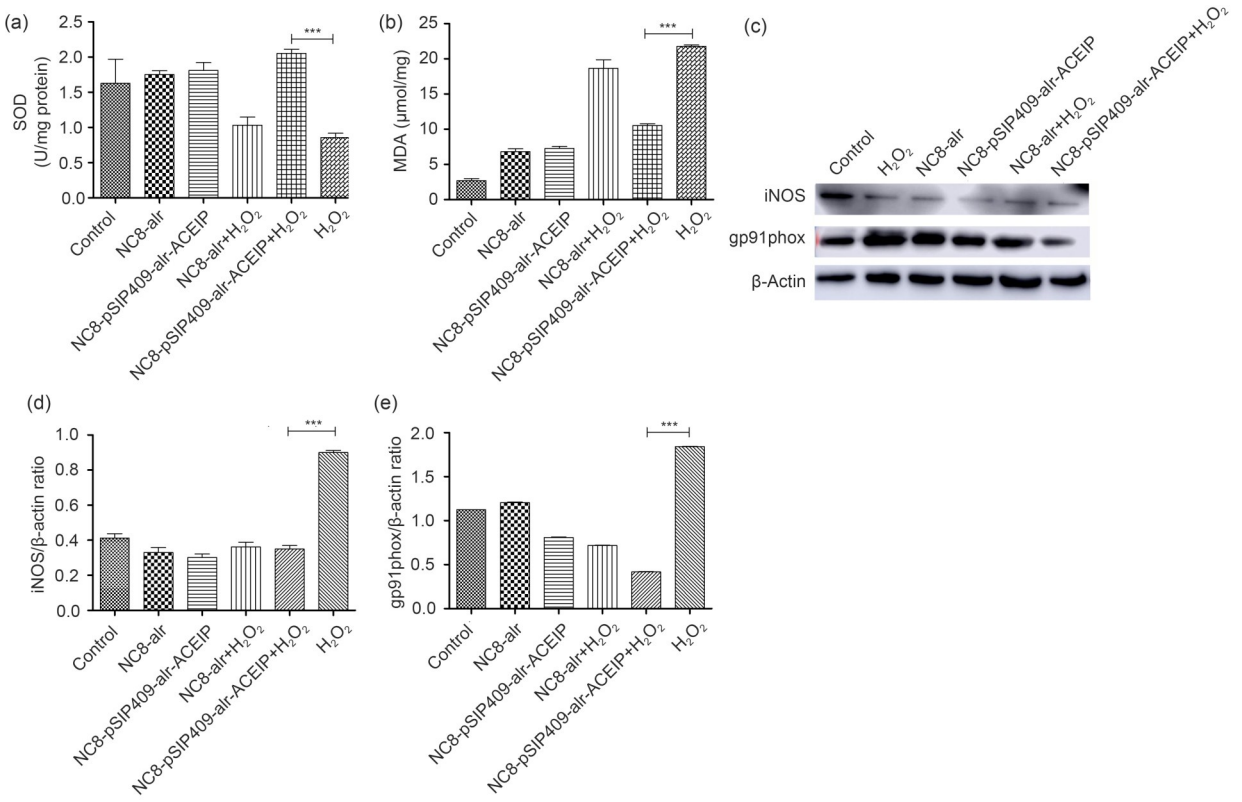

Fig. 8 Effects of NC8-pSIP409-alr-ACEIP on anti-oxidation-related indicators. (a) SOD activity in Hy-HUVEC cells. (b) MDA content of Hy-HUVEC cells. (c) Protein profiles of iNOS, gp91phox, and β-actin. β-Actin used as an internal control, and the induced cells were harvested by centrifugation at 1500 r/min for 3 min at 4 °C and suspended in 50 mmol/L PBS, followed by sonic disruption. The cell-free extract was analyzed on 12% SDS-PAGE and subjected to western blotting using iNOS rabbit polyclonal antibody, gp91phox rabbit polyclonal antibody, and β-actin mouse monoclonal antibody. (d) The ratio of iNOS protein to β-actin. (e) The ratio of gp91phox protein to β-actin. Results are expressed as mean±SEM (n=3). $^{***}P$<0.001, compared with the H_2O_2 positive control group, according to ANOVA. Hy-HUVEC: H_2O_2-induced human umbilical vein endothelial cell; ACEIP: angiotensin-converting enzyme inhibitory peptide; SOD: superoxide dismutase; MDA: malondialdehyde; iNOS: inducible nitric oxide synthase; gp91phox: nicotinamide adenine dinucleotide phosphate oxidase 2; SDS-PAGE: sodium dodecyl sulfate-polyacrylamide gel electrophoresis; SEM: standard error of the mean; ANOVA: analysis of variance.

distributed in a variety of non-phagocytic cells in vivo. Zeng et al. (2019) suggested that the core structural protein gp91phox is the main source of ROS. Wasilewska et al. (2013) showed that the expression of gp91phox and iNOS decreased with increasing AngII levels during cardiovascular disease. The iNOS and gp91phox proteins in Hy-HUVEC cells supplemented with NC8-pSIP409-alr-ACEIP were significantly lower than those in the NC8-alr experimental group (Figs. 8c–8e). Therefore, NC8-pSIP409-alr-ACEIP increased the activity of SOD and decreased the content of MDA in Hy-HUVEC, and simultaneously reduced the expression levels of iNOS and gp91phox proteins, indicating that NC8-pSIP409-alr-ACEIP has a good anti-oxidation effect.

3.9 Effects of NC8-pSIP409-alr-ACEIP on apoptosis-related protein expression and activity in HUVEC cells

To further demonstrate the apoptotic mechanisms of Hy-HUVEC cells induced by NC8-pSIP409-alr-ACEIP, we investigated the expression levels and activity of proteins associated with cell apoptosis (Figs. 9a–9g). After treatment with NC8-pSIP409-alr-ACEIP (160:1) for 2 h, the cells were lysed for western blotting analysis. The results clearly demonstrated that Bcl-2 was increased and Bax was reduced in the Hy-HUVEC cells, compared with the positive control group (Figs. 9a–9d). Activities of caspase-3, -8, and -9 were also determined by colorimetric assays

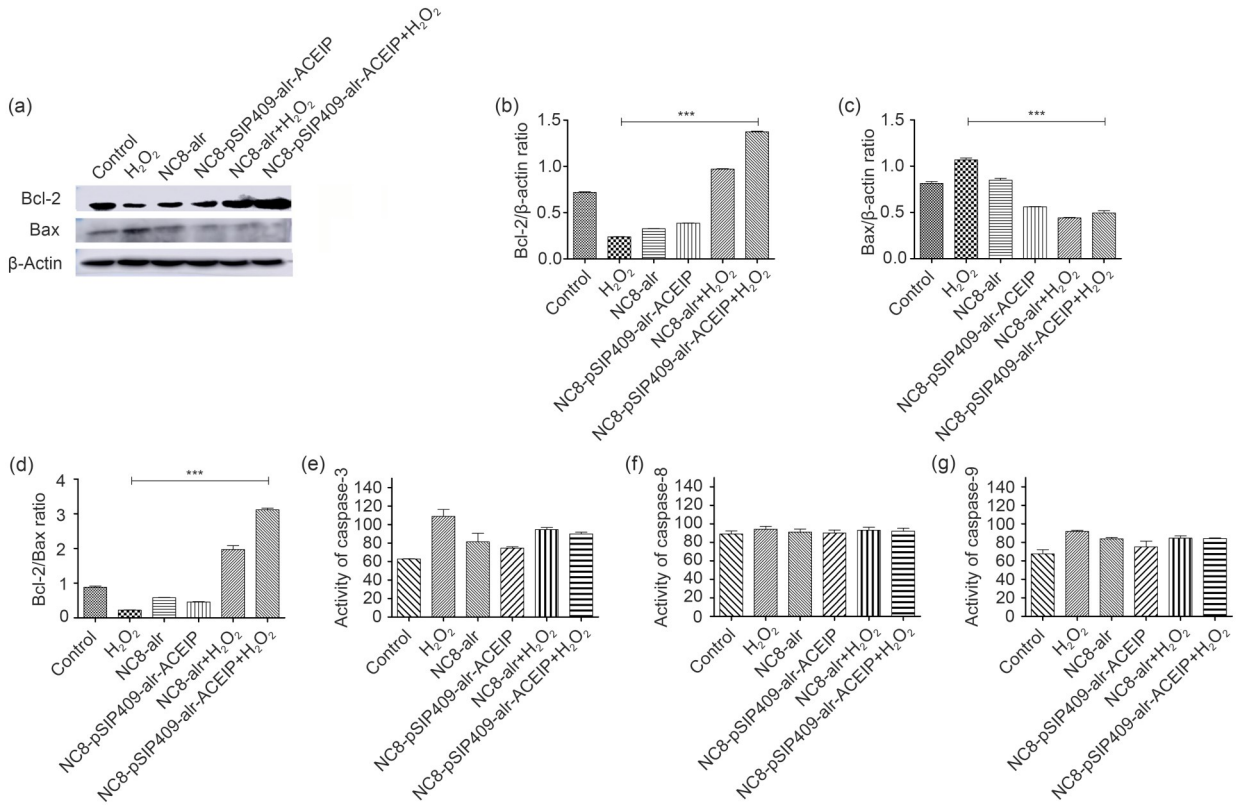

Fig. 9 Detection of HUVEC cell apoptosis-related protein expression and activity by NC8-pSIP409-alr-ACEIP. (a) Protein profiles of Bcl-2, Bax, and β-actin. β-Actin was used as an internal control, and the induced cells were harvested by centrifugation at 1500 r/min for 3 min at 4 °C and were suspended in 50 mmol/L PBS, followed by sonic disruption. The cell-free extract was analyzed on 12% SDS-PAGE and subjected to western blotting using Bal-2 rabbit polyclonal antibody, Bax rabbit polyclonal antibody, and β-actin mouse monoclonal antibody. (b) The ratio of Bcl-2 to β-actin. (c) The ratio of Bax to β-actin. (d) The ratio of Bcl-2 to Bax. (e–g) Equal amounts of cell lysates were assayed for caspase-3 (e), -8 (f), and -9 (g) activity using DEVD-pNA, IETD-pNA, and LEHD-pNA as substrates, respectively. The concentrations of fluorescent products released were measured immediately at 405 nm using a microplate reader. Results represent the mean±standard deviation (SD) of triplicate assays. *** $P<0.001$, compared with the H_2O_2 positive control group, according to ANOVA. ACEIP: angiotensin-converting enzyme inhibitory peptide; Bcl-2: B-cell lymphoma 2; Bax: Bcl-2-associated X protein; SDS-PAGE: sodium dodecyl sulfate-polyacrylamide gel electrophoresis; Ac-DEVD-pNA: acetyl-Asp-Glu-Val-Asp-p-nitroanilide; Ac-IETD-pNA: acetyl-Ile-Glu-Thr-Asp-p-nitroanilide; Ac-LEHD-pNA: acetyl-Leu-Glu-His-Asp-p-nitroanilide; ANOVA: analysis of variance.

(Figs. 9e−9g). Activities of caspase-3 and -9 were reduced in Hy-HUVEC cells, compared with the positive control group (Figs. 9e and 9g); caspase-8 activity showed no significant change (Fig. 9f). These observations suggested that Hy-HUVEC cells were effectively protected and that apoptosis was reduced by NC8-pSIP409-alr-ACEIP through a caspase-dependent pathway.

3.10 Effects of NC8-pSIP409-alr-ACEIP on expression levels of AngII and ACE2 proteins associated with hypertension

Since NC8-pSIP409-alr-ACEIP cells express the ACEIP fusion protein with a hypotensive effect, we explored the changes in intracellular AngII and ACE2 proteins in Hy-HUVEC cells treated with NC8-pSIP409-alr-ACEIP. After adding NC8-pSIP409-alr-ACEIP to Hy-HUVEC cells for 2 h with a ratio of 160:1, the expression of AngII protein was significantly lower than that of the H_2O_2 positive control group, but significantly higher than that of the NC8-alr experimental group. The expression of ACE2 protein in the H_2O_2 positive control group was absent compared to the control group. However, the expression of ACE2 protein significantly increased after addition of NC8-pSIP409-alr-ACEIP (Fig. 10). These results further confirmed the hypothesis that NC8-pSIP409-alr-ACEIP has a beneficial effect on reducing hypertension.

4 Discussion

This study focused on the damage effect of HUVEC in hypertension from the perspective of apoptosis and oxidative stress. Our work also explored the possible mechanism of action of a novel functional recombinant *L. plantarum* NC8-pSIP409-alr-ACEIP in reducing blood pressure.

Vaziri et al. (2000) constructed an oxidative stress model by feeding rats with glutathione synthetase inhibitors, and simultaneously compared the effects of treatment with antioxidants to placebo. As shown in the results, the placebo-treated rats developed persistent hypertension and the antioxidant-treated rats showed a blood pressure drop, but the antioxidant treatment had no significant effect on the blood pressure of normal rats. After the construction of an oxidative stress model, Vaziri et al. (2000) found that ROS could cause hypertension, which was confirmed from another perspective that hypertension is associated with ROS. Wang et al. (2016) constructed an oxidative stress model in H_2O_2-induced endothelial cells; this study has shown that it is feasible to construct a hypertensive cell model by inducing HUVEC cells with H_2O_2. We have found that different concentrations of H_2O_2 could reduce the survival rate of HUVEC cells to different degrees, with a dose- and time-dependent relationship (Fig. 2). Pre-protecting Hy-HUVEC by incubating these cells with

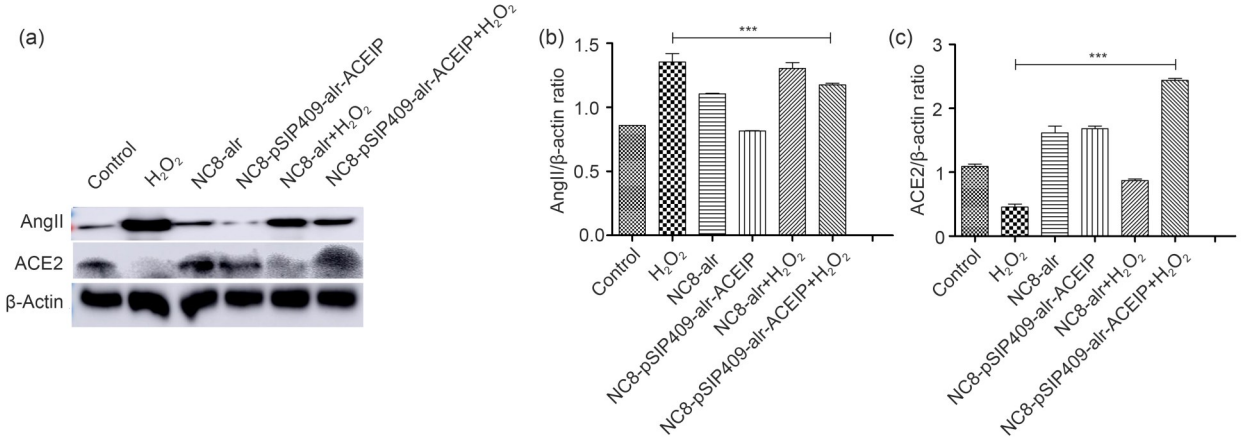

Fig. 10 Effects of NC8-pSIP409-alr-ACEIP on AngII and ACE2 protein expression levels. (a) Protein profiles of AngII, ACE2, and β-actin. β-Actin was used as an internal control, and the induced cells were harvested by centrifugation at 1500 r/min for 3 min at 4 °C and were suspended in 50 mmol/L PBS, followed by sonic disruption. The cell-free extract was analyzed on 15% SDS-PAGE and subjected to western blotting using angiopoietin 2 rabbit polyclonal antibody, ACE2 rabbit polyclonal antibody, and β-actin mouse monoclonal antibody. (b) The ratio of AngII to β-actin. (c) The ratio of ACE2 to β-actin. Results represent the mean±standard deviation (SD) of triplicate assays. *** P<0.001, compared with the H_2O_2 positive control group according to ANOVA. ACEIP: angiotensin-converting enzyme inhibitory peptide; SDS-PAGE: sodium dodecylsulfate-polyacrylamide gel electrophoresis; ACE2: angiotensin-converting enzyme 2; ANOVA: analysis of variance.

different NC8-pSIP409-alr-ACEIP/cell ratios for 2 h, the cell survival rate was increased significantly. At a ratio of 160:1, the survival rate increased by nearly 20% (Fig. 4). For experimental purposes, this study also verified that NC8-pSIP409-alr-ACEIP is not toxic to HUVEC (Fig. 3). Liu et al. (2011) found that *Lactobacillus casei* 01 after heat treatment could inhibit the apoptosis of human intestinal epithelial cells, intestinal 407 cells, and human colon cancer cells HT-29, thereby exerting a role in cell proliferative effect. Deepak et al. (2016) and Santos et al. (2016) also demonstrated that lactic acid bacteria have an inhibitory effect on apoptosis. In our study, the results of FCM also showed that the protective effect of NC8-pSIP409-alr-ACEIP could effectively reduce apoptosis of Hy-HUVEC (Fig. 5). Bax and Bcl-2 are the key proteins for apoptosis, and their ratio is often used as an indicator of cell survival potential (Chen et al., 2004; Bian et al., 2011). Du et al. (2016) demonstrated that blueberry anthocyanins reduced expression of the apoptotic proteins Bax and Bcl-2, thereby inhibiting apoptosis of endothelial cells. At the same time, the low expression of Bcl-2 protein can lead to the reduction of antioxidant (Huang et al., 2006). Białas et al. (2016) and Ott et al. (2007) have suggested that apoptosis could cause an increase in ROS content and an imbalance in Bcl-2 and Bax. An increase in Bax protein expression in mitochondria will lead to a decrease in intracellular MMP; subsequently, cytochrome *c* released in mitochondria enters the cytoplasm and binds to caspase-9 to form a complex that activates caspase-3 and triggers apoptosis (Ott et al., 2007; Białas et al., 2016; Zhang SS et al., 2016). As shown in Fig. 9, NC8-pSIP409-alr-ACEIP increased the Bcl-2/Bax ratio in Hy-HUVEC and decreased caspase-3 and caspase-9 activity, but showed no effect on caspase-8 activity. In addition, MMP began to repolarize and gradually returned to normal (Fig. 7).

MDA indirectly reflects the degree of cell damage by reflecting the degree of lipid peroxidation in cells. In addition, SOD is a key enzyme that balances oxidation and anti-oxidation of the body, and it can remove superoxide anion radicals and protect cells from damage (Maghraoui et al., 2014; Camini et al., 2017). In addition, changes in iNOS and gp91phox protein expression levels regulate oxidative stress, thereby inhibiting apoptosis (Lee et al., 2015; Luo et al., 2015). Extracting *Lactobacillus fermentum* E-3 and E-18 from the intestinal flora of healthy children, Sharafedtinov et al. (2013) demonstrated the antioxidant effects of lactic acid bacteria by determining ROS and SOD, which is consistent with the results in this study. In our study, NC8-pSIP409-alr-ACEIP protected Hy-HUVEC cells, showing a decrease in ROS content (Fig. 6), expression of iNOS and gp91phox proteins, and MDA content (Fig. 8), coupled with an increase in SOD activity. More importantly, our data analysis clearly indicated the advantages of NC8-pSIP409-alr-ACEIP. In each experiment, we have separately tested NC8-alr as a negative control group. Although the NC8-alr group also reduced apoptosis and decreased intracellular oxidative stress, its effect was significantly lower than that of the NC8-pSIP409-alr-ACEIP group.

In the brain, AngII protein plays a very important role in mediating neuropathic hypertension. In particular, the AngII protein produced around and locally in the brain can induce hypertension by regulating redox levels, endoplasmic reticulum (ER), inflammation, and transcription factor pathways in the brain (Young and Davisson, 2015; Collister et al., 2016). Activation of RAS is an important mechanism for activation of NADPH oxidase and the production of ROS during hypertension. AngII produces ROS mainly by mediating type I receptors, and NADPH oxidase and related subunits show a significant decrease in expression after the addition of AT1 receptor antagonists (Bali et al., 2014). Oxidative stress leads to an increase in ROS with HUVEC apoptosis (Wali et al., 2014). Moreover, H_2O_2 can reduce expression of ACE2 protein and increase the expression of AngII protein, thereby engendering a state of hypertension in cells, and eventually leading to apoptosis. In this study, we found that addition of NC8-pSIP409-alr-ACEIP deceased the expression of AngII protein and increased protein expression of ACE2 (Fig. 10). The above analyses definitively demonstrated that NC8-pSIP409-alr-ACEIP can decrease the apoptotic rate of vascular endothelial cells under high blood pressure by reducing oxidative stress in cells, thereby reducing hypertension. It is worth mentioning that unlike the previous construction of a pSIP-409-ACEIP strain by Yang GL et al. (2015), the recombinant *L. plantarum* constructed in this study was replaced with non-resistant carriers, which improved biosafety. This large advance offers new possibilities for further research and development of health-care foods with strong antihypertensive effects, high safety, and low toxicity.

With increasing awareness of and demand for *L. plantarum*, the development of various functional oral preparations of *L. plantarum* has become a topic of significant research interest. From the perspective of nutrition, the future development trend is that under the control of nutritional balance, disease will be gradually reduced. The blood pressure-reducing recombinant *L. plantarum* used in this study is in line with this trend. In future investigations, we plan to conduct in vivo research in SHR rats. Since the *Lactobacillus* strain in this study is food-grade, we intend to ferment this bacterium as yogurt or as *Lactobacillus* tablets as part of future small-scale clinical experiments. It is hoped that this strain of lactic acid bacteria can be commercialized to benefit hypertension patients around the world.

Acknowledgments

This work is supported the National Key Research and Development Program of China (Nos. 2017YFD0501000 and 2017YFD0501200), the National Natural Science Foundation of China (Nos. 31672528, 31941018, and 32072888), the Science and Technology Project of Jilin Provincial Department of Education (No. JJKH20190942KJ), and the Science and Technology Development Program of Jilin Province (Nos. 20180201040NY and 20190301042NY), China.

Author contributions

Guan WANG and Mingyue HAO performed the experimental research and data analysis, and wrote and edited the manuscript. Mingyue HAO performed the establishment of cell models. Qiong LIU, Yanlong JIANG, and Haibin HUANG contributed to the study design, data analysis, and writing and editing of the manuscript. Guilian YANG and Chunfeng WANG performed experimental design. All authors have read and approved the final manuscript and, therefore, have full access to all the data in the study and take responsibility for the integrity and security of the data.

Compliance with ethics guidelines

Guan WANG, Mingyue HAO, Qiong LIU, Yanlong JIANG, Haibin HUANG, Guilian YANG, and Chunfeng WANG declare that they have no conflict of interest.

This article does not contain any studies with human or animal subjects performed by any of the authors.

References

Aldabbous L, Abdul-Salam V, McKinnon T, et al., 2016. Neutrophil extracellular traps promote angiogenesis. *Arterioscler Thromb Vasc Biol*, 36(10):2078-2087. https://doi.org/10.1161/ATVBAHA.116.307634

Bali A, Singh N, Jaggi AS, 2014. Renin-angiotensin system in pain: existing in a double life? *J Renin Angiotensin Aldosterone Syst*, 15(4):329-340. https://doi.org/10.1177/1470320313503694

Białas AJ, Sitarek P, Miłkowska-Dymanowska J, et al., 2016. The role of mitochondria and oxidative/antioxidative imbalance in pathobiology of chronic obstructive pulmonary disease. *Oxid Med Cell Longev*, 2016:7808576. https://doi.org/10.1155/2016/7808576

Bian YF, Yang HY, Yang ZM, et al., 2011. Amlodipine treatment prevents angiotensin II-induced human umbilical vein endothelial cell apoptosis. *Arch Med Res*, 42(1):22-27. https://doi.org/10.1016/j.arcmed.2011.01.012

Camini FC, da Silva Caetano CC, Almeida LT, et al., 2017. Oxidative stress in *Mayaro virus* infection. *Virus Res*, 236:1-8. https://doi.org/10.1016/j.virusres.2017.04.017

Chen JW, Mehta JL, Haider N, et al., 2004. Role of caspases in Ox-LDL-induced apoptotic cascade in human coronary artery endothelial cells. *Circ Res*, 94(3):370-376. https://doi.org/10.1161/01.RES.0000113782.07824.BE

Collister JP, Taylor-Smith H, Drebes D, et al., 2016. Angiotensin II-induced hypertension is attenuated by overexpressing copper/zinc superoxide dismutase in the brain organum vasculosum of the lamina terminalis. *Oxid Med Cell Longev*, 2016:3959087. https://doi.org/10.1155/2016/3959087

Deepak V, Ramachandran S, Balahmar RM, et al., 2016. In vitro evaluation of anticancer properties of exopolysaccharides from *Lactobacillus acidophilus* in colon cancer cell lines. *In Vitro Cell Dev Biol Anim*, 52(2):163-173. https://doi.org/10.1007/s11626-015-9970-3

Du J, Leng JY, Zhang L, et al., 2016. Angiotensin II-induced apoptosis of human umbilical vein endothelial cells was inhibited by blueberry anthocyanin through Bax- and Caspase 3-dependent pathways. *Med Sci Monit*, 22:3223-3228. https://doi.org/10.12659/MSM.896916

Ettinger G, MacDonald K, Reid G, et al., 2014. The influence of the human microbiome and probiotics on cardiovascular health. *Gut Microbes*, 5(6):719-728. https://doi.org/10.4161/19490976.2014.983775

Fraga-Silva RA, Costa-Fraga FP, Murça TM, et al., 2013. Angiotensin-converting enzyme 2 activation improves endothelial function. *Hypertension*, 61(6):1233-1238. https://doi.org/10.1161/HYPERTENSIONAHA.111.00627

Gordon JI, 2012. Honor thy gut symbionts redux. *Science*, 336(6086):1251-1253. https://doi.org/10.1126/science.1224686

Graham D, Hamilton C, Beattie E, et al., 2004. Comparison of the effects of omapatrilat and irbesartan/hydrochlorothiazide on endothelial function and cardiac hypertrophy in the stroke-prone spontaneously hypertensive rat: sex differences. *J Hypertens*, 22(2):329-337. https://doi.org/10.1097/00004872-200402000-00017

Huang H, Shan J, Pan XH, et al., 2006. Carvedilol protected diabetic rat hearts via reducing oxidative stress. *J Zhejiang Univ-Sci B (Biomed & Biotechnol)*, 7(9):725-731. https://doi.org/10.1631/jzus.2006.B0725

Kim S, Goel R, Kumar A, et al., 2018. Imbalance of gut microbiome and intestinal epithelial barrier dysfunction in

patients with high blood pressure. *Clin Sci*, 132(6):701-718. https://doi.org/10.1042/CS20180087

Korsager Larsen M, Matchkov VV, 2016. Hypertension and physical exercise: the role of oxidative stress. *Medicina*, 52(1):19-27. https://doi.org/10.1016/j.medici.2016.01.005

Laurent S, 2017. Antihypertensive drugs. *Pharmacol Res*, 124:116-125. https://doi.org/10.1016/j.phrs.2017.07.026

Lee EJ, Ko HM, Jeong YH, et al., 2015. β-Lapachone suppresses neuroinflammation by modulating the expression of cytokines and matrix metalloproteinases in activated microglia. *J Neuroinflammation*, 12:133. https://doi.org/10.1186/s12974-015-0355-z

Liu CT, Chu FJ, Chou C, et al., 2011. Antiproliferative and anticytotoxic effects of cell fractions and exopolysaccharides from *Lactobacillus casei* 01. *Mutat Res Genet Toxicol Environ Mutagen*, 721(2):157-162. https://doi.org/10.1016/j.mrgentox.2011.01.005

Liu J, Zhang FF, Li L, et al., 2013. ClC-3 deficiency prevents apoptosis induced by angiotensin II in endothelial progenitor cells via inhibition of NADPH oxidase. *Apoptosis*, 18(10):1262-1273. https://doi.org/10.1007/s10495-013-0881-z

Loperena R, Harrison DG, 2017. Oxidative stress and hypertensive diseases. *Med Clin North Am*, 101(1):169-193. https://doi.org/10.1016/j.mcna.2016.08.004

Lugo-Baruqui A, Muñoz-Valle JF, Arévalo-Gallegos S, et al., 2010. Role of angiotensin II in liver fibrosis-induced portal hypertension and therapeutic implications. *Hepatol Res*, 40(1):95-104. https://doi.org/10.1111/j.1872-034X.2009.00581.x

Luo CF, Yuan DD, Zhao WC, et al., 2015. Sevoflurane ameliorates intestinal ischemia-reperfusion-induced lung injury by inhibiting the synergistic action between mast cell activation and oxidative stress. *Mol Med Rep*, 12(1):1082-1090. https://doi.org/10.3892/mmr.2015.3527

Maghraoui S, Clichici S, Ayadi A, et al., 2014. Oxidative stress in blood and testicle of rat following intraperitoneal administration of aluminum and indium. *Acta Physiol Hung*, 101(1):47-58. https://doi.org/10.1556/aphysiol.100.2013.021

Mendell JT, Olson EN, 2012. MicroRNAs in stress signaling and human disease. *Cell*, 148(6):1172-1187. https://doi.org/10.1016/j.cell.2012.02.005

Ott M, Gogvadze V, Orrenius S, et al., 2007. Mitochondria, oxidative stress and cell death. *Apoptosis*, 12(5):913-922. https://doi.org/10.1007/s10495-007-0756-2

Pavli F, Tassou C, Nychas GJE, et al., 2018. Probiotic incorporation in edible films and coatings: bioactive solution for functional foods. *Int J Mol Sci*, 19(1):150. https://doi.org/10.3390/ijms19010150

Präbst K, Engelhardt H, Ringgeler S, et al., 2017. Basic colorimetric proliferation assays: MTT, WST, and resazurin. *Methods Mol Biol*, 1601:1-17. https://doi.org/10.1007/978-1-4939-6960-9_1

Santos CMA, Pires MCV, Leão TL, et al., 2016. Selection of *Lactobacillus* strains as potential probiotics for vaginitis treatment. *Microbiology*, 162(7):1195-1207. https://doi.org/10.1099/mic.0.000302

Sharafedtinov KK, Plotnikova OA, Alexeeva RI, et al., 2013. Hypocaloric diet supplemented with probiotic cheese improves body mass index and blood pressure indices of obese hypertensive patients—a randomized double-blind placebo-controlled pilot study. *Nutr J*, 12:138. https://doi.org/10.1186/1475-2891-12-138

Shreiber DI, Enever PAJ, Tranquillo RT, 2001. Effects of PDGF-BB on rat dermal fibroblast behavior in mechanically stressed and unstressed collagen and fibrin gels. *Exp Cell Res*, 266(1):155-166. https://doi.org/10.1006/excr.2001.5208

Small HY, Migliarino S, Czesnikiewicz-Guzik M, et al., 2018. Hypertension: focus on autoimmunity and oxidative stress. *Free Radic Biol Med*, 125:104-115. https://doi.org/10.1016/j.freeradbiomed.2018.05.085

Upadrasta A, Madempudi RS, 2016. Probiotics and blood pressure: current insights. *Integr Blood Press Control*, 9:33-42. https://doi.org/10.2147/IBPC.S73246

van Thiel BS, van der Pluijm I, te Riet L, et al., 2015. The renin-angiotensin system and its involvement in vascular disease. *Eur J Pharmacol*, 763:3-14. https://doi.org/10.1016/j.ejphar.2015.03.090

Vaziri ND, Wang XQ, Oveisi F, et al., 2000. Induction of oxidative stress by glutathione depletion causes severe hypertension in normal rats. *Hypertension*, 36(1):142-146. https://doi.org/10.1161/01.HYP.36.1.142

Wali JA, Rondas D, McKenzie MD, et al., 2014. The proapoptotic BH3-only proteins Bim and Puma are downstream of endoplasmic reticulum and mitochondrial oxidative stress in pancreatic islets in response to glucotoxicity. *Cell Death Dis*, 5(3):e1124. https://doi.org/10.1038/cddis.2014.88

Wan L, Nie GJ, Zhang J, et al., 2011. β-Amyloid peptide increases levels of iron content and oxidative stress in human cell and *Caenorhabditis elegans* models of Alzheimer disease. *Free Radic Biol Med*, 50(1):122-129. https://doi.org/10.1016/j.freeradbiomed.2010.10.707

Wang JY, Sun PP, Bao YM, et al., 2012. Vitamin E renders protection to PC12 cells against oxidative damage and apoptosis induced by single-walled carbon nanotubes. *Toxicol in Vitro*, 26(1):32-41. https://doi.org/10.1016/j.tiv.2011.10.004

Wang ZX, Wang Y, Chen YF, et al., 2016. The IL-24 gene protects human umbilical vein endothelial cells against H_2O_2-induced injury and may be useful as a treatment for cardiovascular disease. *Int J Mol Med*, 37(3):581-592. https://doi.org/10.3892/ijmm.2016.2466

Wasilewska E, Złotkowska D, Pijagin ME, 2013. The role of intestinal microflora and probiotic bacteria in prophylactic and development of colorectal cancer. *Postepy Hig Med Dosw*, 67:837-847. https://doi.org/10.5604/17322693.1061847

Wu Q, Liu XX, Lu DY, et al., 2018. Protective effect of polygonum orientale flower extract on H_2O_2-induced oxidative damage of HUVEC cells. *China J Chin Mat Med*, 43(5):1008-1013 (in Chinese).

https://doi.org/10.19540/j.cnki.cjcmm.2018.0033

Wu YC, Wang YM, Nabi X, 2019. Protective effect of *Ziziphora clinopodioides* flavonoids against H_2O_2-induced oxidative stress in HUVEC cells. *Biomed Pharmacother*, 117: 109156.
https://doi.org/10.1016/j.biopha.2019.109156

Yang GL, Jiang YL, Yang WT, et al., 2015. Effective treatment of hypertension by recombinant *Lactobacillus plantarum* expressing angiotensin converting enzyme inhibitory peptide. *Microb Cell Fact*, 14:202.
https://doi.org/10.1186/s12934-015-0394-2

Yang T, Santisteban MM, Rodriguez V, et al., 2015. Gut dysbiosis is linked to hypertension. *Hypertension*, 65(6):1331-1340.
https://doi.org/10.1161/HYPERTENSIONAHA.115.05315

Young CN, Davisson RL, 2015. Angiotensin-II, the brain, and hypertension. *Hypertension*, 66(5):920-926.
https://doi.org/10.1161/HYPERTENSIONAHA.115.03624

Zeng MY, Miralda I, Armstrong CL, et al., 2019. The roles of NADPH oxidase in modulating neutrophil effector responses. *Mol Oral Microbiol*, 34(2):27-38.
https://doi.org/10.1111/omi.1225

Zhang SS, Qin FX, Yang LY, et al., 2016. Nucleophosmin mutations induce chemosensitivity in THP-1 leukemia cells by suppressing NF-κB activity and regulating Bax/Bcl-2 expression. *J Cancer*, 7(15):2270-2279.
https://doi.org/10.7150/jca.16010

Zhang Y, Zou CS, Yang SW, et al., 2016. p120 catenin attenuates the angiotensin II-induced apoptosis of human umbilical vein endothelial cells by suppressing the mitochondrial pathway. *Int J Mol Med*, 37(3):623-630.
https://doi.org/10.3892/ijmm.2016.2476

Zhou B, Bentham J, di Cesare M, et al., 2017. Worldwide trends in blood pressure from 1975 to 2015: a pooled analysis of 1479 population-based measurement studies with 19·1 million participants. *Lancet*, 389(10064):37-55.
https://doi.org/10.1016/S0140-6736(16)31919-5

Zittermann A, Pilz S, 2019. Vitamin D and cardiovascular disease: an update. *Anticancer Res*, 39(9):4627-4635.
https://doi.org/10.21873/anticanres.13643